Desalination and Water Treatment
www.deswater.com

doi:10.5004/dwt.2019.23904

153 (2019) 312–320
June

Decolorization of triphenylmethane dyes and dye-doped silica microspheres using sodium percarbonate

Jun Zhang*, Xiaoli Wang, Chuan Dong

Institute of Environmental Science, Shanxi University Taiyuan, China, Tel. +86 0351-7011011, email: dc104@sxu.edu.cn (J. Zhang), 859594114@qq.com (X. Wang), dc@sxu.edu.cn (C. Dong)

Received 17 May 2018; Accepted 1 February 2019

ABSTRACT

Three triphenylmethane (TPM) dyes, namely brilliant green, basic fuchsin, and crystal violet were decolorized using sodium percarbonate (SPC) in the practical decolorization of TPM dyes in wastewater. The decolorization conditions such as pH, temperature, bleaching time and the dosage of oxidant were examined based on the decolorization percentage change. Under the optimal conditions, the decolorization percentage of three TPM dyes averagely reaches around 90% in 20 min at pH 11 and room temperature (20°C). The optimal dosage of SPC was determined for the three TPM dyes respectively. The TPM-doped silica microspheres were synthesized by the Stöber method and characterized by UV-Vis, IR, and TEM techniques. The synthesized TPM@SiO_2 microspheres were also decolorized effectively by sodium percarbonate. The degradation mechanism of the amino- or alkylamino-TPM dyes is proposed based on the UV-Vis analyzes, by which the degradation process could undergo two dominant reactions: the destruction of conjugated structure and N-dealkylation reaction. This study verifies the viability of the use of sodium percarbonate for the wastewater treatment of TPM dyes.

Keywords: Triphenylmethane dyes; Sodium percarbonate; Decolorization; Degradation mechanism; Silica microspheres

1. Introduction

Triphenylmethane (TPM) dyes are widely used in textile dyeing, paper, and printing industry. The environmental residue and pollution control of TPM dyes and their degradation products have aroused widespread public concern. Doping with silica nanoparticles is an efficient way to improve the water solubility, stability, and biocompatibility of dyes [1]. The toxicity of the dyes can be reduced greatly by the strong electrostatic adsorption between dyes and SiO_2 nanoparticles [2]. In recent years, the methods of combining inorganic silica with organic dyes have been widely developed including covalent coupling [3], electrostatic adsorption [4], and reverse microemulsion method [5], in which the electrostatic adsorption is accepted as an optimal method. By doping with silica, TPM dyes are spread to more field and get more extensive applications such as being adsorbent in textile dyeing [6], being pigments in printing industry [7,8].

The chemical degradation including oxidation, reduction, and electrochemical degradation is widely adopted for destructing the conjugated structure of TPM dyes [9,10]. The oxidation degradation has developed from the classical Fenton method to photocatalytic oxidation [11], microwave or ultrasonic-assisted oxidation [12] etc., in which hydrogen peroxide (HP) is a commonly used oxidant [13,14]. In addition, the oxidative degradation of TPM dyes has also been carried out using high valence oxides such as potassium ferrate [15], potassium persulfate [16]. Electrochemical methods are often used to degrade TPM dyes [17,18]. In general, the mechanism of oxidative degradation to TPM dyes has focused on the attack of carbon cations by hydroxyl radicals, which is roughly explained as the competition of two

---

*Corresponding author.

1944-3994 / 1944-3986

reactions, the cleavage of the central carbon reaction and N-dealkylation [19].

In the oxidation degradation of dyes, HP has the disadvantages of poor stability and high cost in transportation and storage. Sodium percarbonate (SPC) has been reported as a solid carrier of HP with the same features as the liquid carrier but having safer handling and environmentally friendly procedures [20,21]. Meanwhile, SPC can also lead to the development of well-known Fenton-like chemistry by disassociating to HP and sodium carbonate when mixed with water, as shown in Eq. (2) ($Na_2CO_3 \cdot 1.5H_2O$) → $2Na_2CO_3 + H_2O_2$, and it offers many of the same functional benefits as liquid HP. SPC has an active available oxygen content which is equivalent to 27.5% H_2O_2.

The oxidation mechanism of organics by SPC is generally believed consistent with that of HP, that is the strong oxidative degradation of organic matter by hydroxyl radicals [22,23]. However, there are significant differences between SPC and HP in the experimental conditions for the functional group oxidation [24]. SPC is suitable for the aqueous solutions in a wider pH range than HP [25]. To our best knowledge, there is a paucity of literature directly related to the degradation of TPM dyes by SPC. The degradation of Rhodamine Bby SPC has been investigated, which shows the reaction principle of SPC and HP is essentially the same [26]. The first-order rate constants have been observed for methylene blue degradation (k_{MB}) by SPC and HP in unbuffered solution. The k_{MB} order of SPC > HP suggests SPC is much more efficient than HP at that condition [27]. In addition, SPC is a partial substitute for sodium hydroxide in bleaching cotton and linen fabrics.

In this paper, using brilliant green (BG), basic fuchsin (BF) and crystal violet (CV), (Fig. 1) as model compounds, the decolorization and degradation of TPM dyes by SPC was detailed studied. The decolorization conditions of three TPM dyes by SPC were optimized. Moreover, to reduce the environmental hazards of TPMs, TPM@SiO_2 microspheres were synthesized and characterized using UV-Vis, IR, and TEM techniques. The TPM@SiO_2 microspheres were also decolorized by SPC. The degradation mechanisms of basic dyes with amino- or alkylamino-TPM structure by SPC are proposed based on the spectra data processing.

2. Experimental

2.1. Apparatus and reagents

The UV-Vis absorption spectra were obtained from a TU-1901 spectrophotometer (Beijing, China). IR spectroscopy was carried out using an FTIR-8000 Infrared spectrometer (Shimadzu, Japan). A JEM-1200EX transmission electron microscope (JEOL) was used for the TEM analysis. The pH of solutions was measured with a Mettler-Toledo FE20 pH-meter (Mettler-Toledo Instruments Co., Ltd., Shanghai).

The dyes of BG($C_{27}H_{34}N_2O_4S$), BF($C_{20}H_{20}ClN_3$) and CV ($C_{25}H_{30}N_3Cl$) were purchased from Sigma Company and used as such without further purification. The initial concentration of dye solution in all experiments was 100 mg/L and the initial concentration of SPC solution was 100 mg/L without special explanations. Double distilled water was used to prepare all the solutions.

2.2. The calculation of decolorization percentage (DP)

According to Lambert-Beer law, good linear fits have been observed between the maximum absorbance value of dye solution and the dye concentration in the range of 1 mg/L to 100 mg/L. Therefore, the followed formula was employed in the calculation of the dye DP: $DP = (1–A/A_0) \times 100\%$. Where A_0, A respectively indicate the maximum absorbance value of the dye solution before and after decolorization. All decolorization experiments were carried out in triplicates and the data values represented as mean ± standard error (S.E.) with S.E. values shown as Y-error bars in all figures.

2.3. Effect of pH on the TPM dyes decolorization by SPC

The buffers of Britton–Robinson (BR) at pH 3–12 were added into 1 mL of the dye solutions. Using the buffer without dye as the reference, the absorbance of each solution was measured and recorded as $A_{3.0}$–$A_{12.0}$ respectively.

A quantity of SPC solution was added into the 1 mL of the dye solution. BR buffers of pH 3–12 were added into

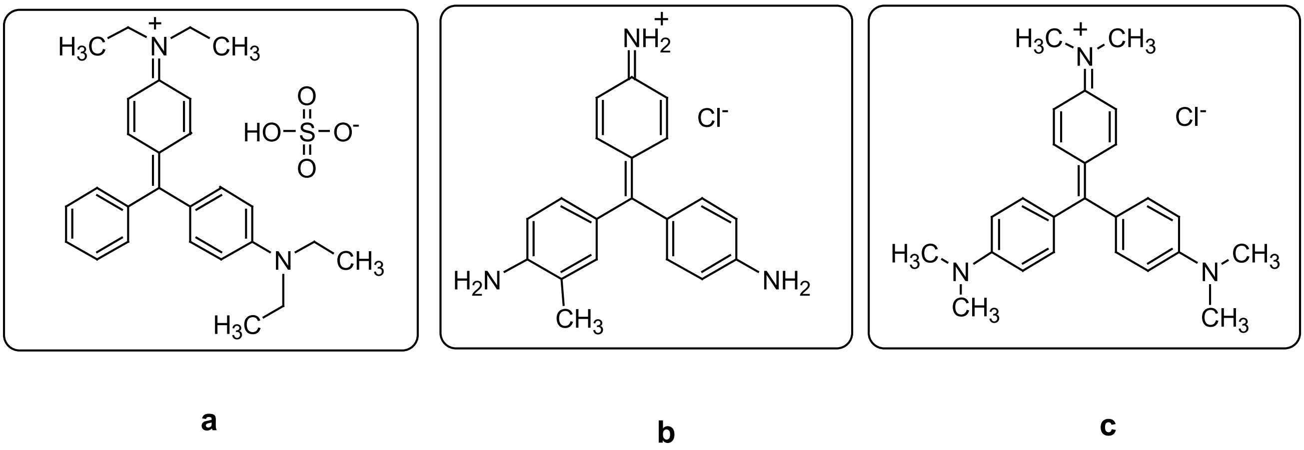

Fig. 1. The structure of three TPM dyes (a. BG, b. BF, c. CV).

the solutions respectively. After 20 min, using the buffer without dye as the reference, the absorbance of each dye solution was measured and recorded as A_3–A_{12} respectively.

2.4. Effect of SPC dose and reaction time on the TPM dyes decolorization by SPC

The solution of SPC (50 mg/L) in different volumes was added into the 1 mL of dye solution respectively. The pH of the solution was adjusted to 11 using a buffer. Using the buffer without dye as the reference, the absorbance of the solution was measured at every 5 min.

2.5. Effect of temperature on the TPM dyes decolorization by SPC

A quantity of SPC solution was added into the 1 mL of the dye solution. The pH of the solution was adjusted to 11 using BR buffer. Using the buffer without dye as the reference, the absorbance of the solution was measured at every 5 min at the different temperature.

2.6. Comparison of the decolorization of TPM dyes and TPM@SiO_2 microspheres

The solution of SPC (1 mL, 50 mg/L) was added into the 10 mL of the dye solution. The pH of the solution was adjusted to 11 using BR buffer. After 20 min, using the buffer without dye as the reference, the absorbance of the dye solution was measured.

The microspheres TPM@SiO_2 (50 mg) were ultrasonically dispersed in BR buffer at pH 11. Then 5 mL of SPC solution was added. After oscillating for 40 min, the absorbance of the solutions was measured.

2.7. The UV-Vis spectra change of TPM dyes by adding SPC

A quantity of SPC solution was added into the dye solution (1 mL, 100 mg/L). Using the buffer without dye as the reference, the absorbance of the solution was measured every 2 min.

2.8. The treatment of artificial wastewater using SPC

The simulated wastewater (100 mL) containing TPM-dyes or dye-doped silica microspheres was added in a 250 mL three-necked flask. The pH value was adjusted to 11 using BR buffers. The sample containing the appropriate concentration of SPC was under magnetic stirring. Throughout the degradation experiment, the sample to be analyzed was withdrawn regularly from the flask and filtered. Then the maximum absorbance of the sample was obtained by UV-Vis spectrophotometer, and the removal efficiency was obtained according to the Lambert-Beer standard curve. The removal efficiency (*E*) of dye was calculated as follows: $E = (C_0 - C_i)/C_0 \times 100\%$, where C_0 is the initial concentration of wastewater containing dye, C_i is the concentration of sample treated under a certain condition. The treatment conditions were as follows: the volume of wastewater was 50 mL containing 100 mg/L dye or dye-doped silica microspheres was 50 mL, pH value was 11.0.

3. Results and discussion

SPC was applied to the decolorization of three types (basic dyes, acid dyes, and reactive dyes) with seventeen kinds of dyes (In Support information). Three basic dyes with amino- or alkylamino-TPM structure, namely BG, BF, and CV were selected due to their marked fading response to SPC (Fig. S1).

In UV-Vis spectra, BG, BF and CV exhibit a major absorption peak at 624 nm, 542 nm and 590 nm respectively with minor absorption peaks in the range of 300–450 nm. An apparent decolorization of dye solution was observed upon the addition of SPC, while the maximum absorbance decreased significantly in the UV-Vis spectra. In the present study, the decolorization of dyes was characterized by the decrease in the maximum absorbance.

3.1. Optimization of conditions for TPM dyes decolorization by SPC

An important parameter in TPM dyes degradation is the pH of the solution since it dictates the charge properties of the dyes and oxidant. The dye DP in 20 min as a function of pH in the aqueous reaction is shown in Fig. 2. As depicted in Fig. 2, the DP of the BG, BF, and CV increase with the increase of pH value, reaching the maximum at about pH 11 and then falling a little. As SPC decomposition is facilitated at high pH, more $H_2O_2$is generated and the follow-up product HOO^- is enriched in aqueous solution as well. In the solution at pH 11, the nucleophile HOO^- is the primary oxidizing species, whereas the cationic alkaline dye mainly shows electrophilicity. It has been suggested that the HOO^- attack on the central carbon of TPM-dye molecular causes the formation of dye radical anion, and in the subsequent reactions the radical anion leads to the decolorization of dye [28]. Based on the above discussion, the pH 11 was employed in this work.

The oxidant concentration plays an important role in the dye oxidation. BG, BF, and CV were decolorized by the different concentration of SPC, which is depicted in Fig. 3.

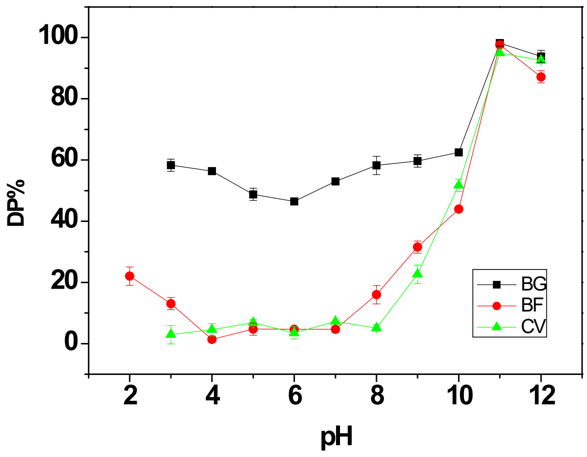

Fig. 2. The effect of pH on the decolorization of TPM dyes (100 mg/L) by SPC (a. BG, b. BF, c. CV).The error bars represent the standard deviation of the replicates (*n* = 3).

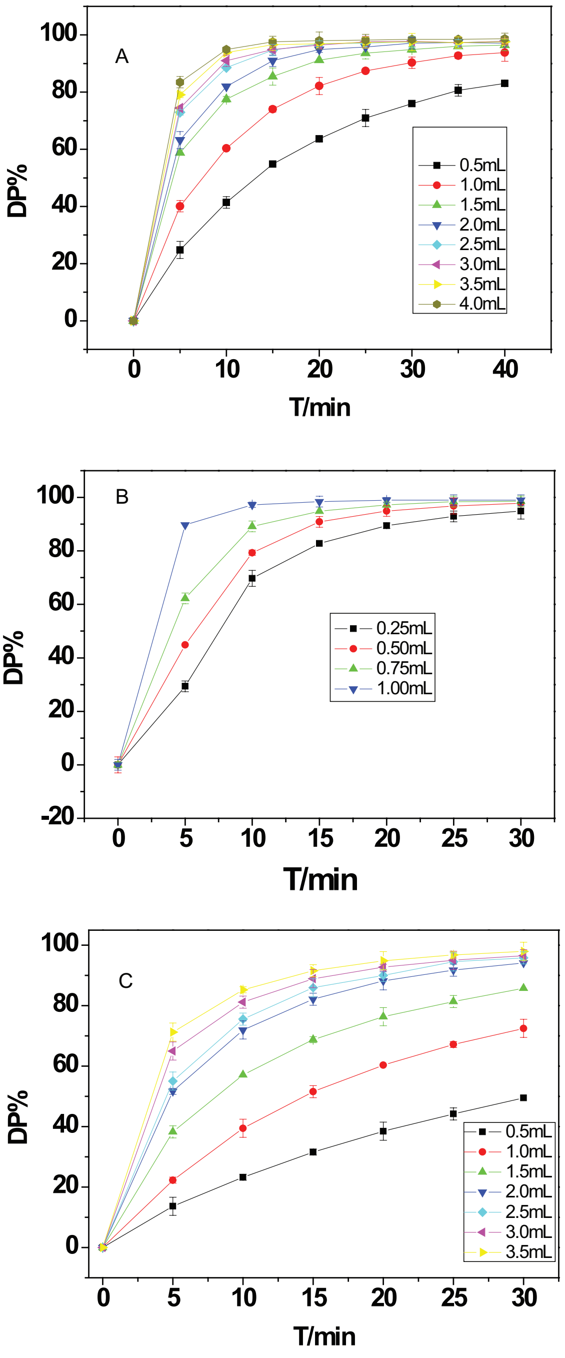

Fig. 3. The effect of SPC dose and reaction time on the decolorization of TPM dyes (a. BG, b. BF, c. CV). The error bars represent the standard deviation of the replicates ($n = 3$).

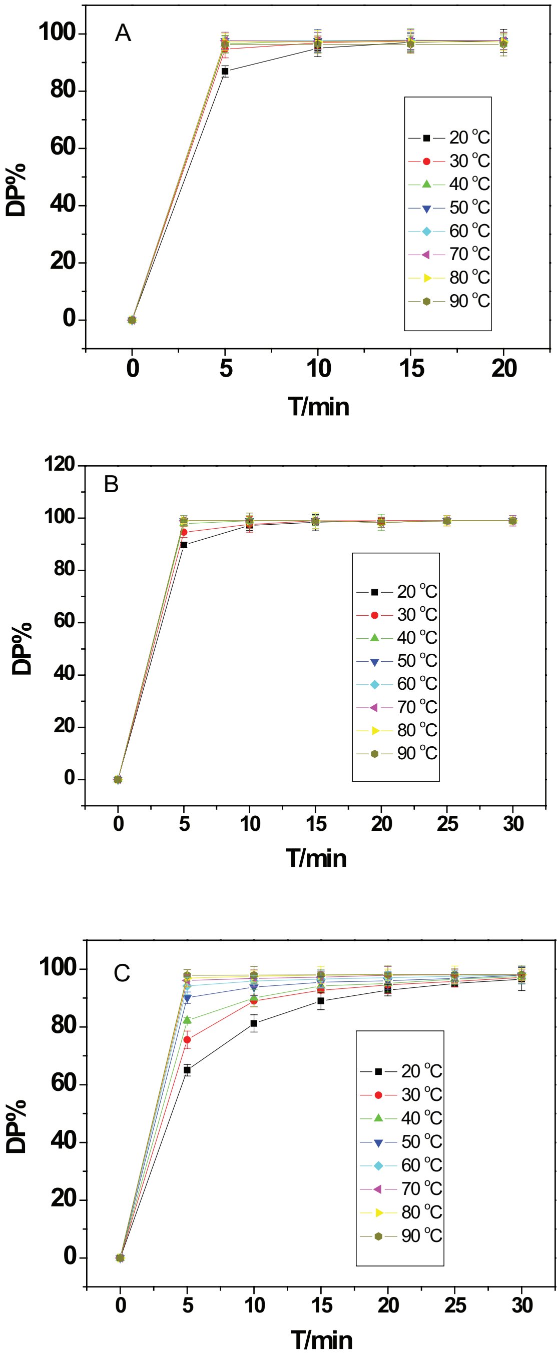

Fig. 4. Temperature effect on the decolorization of TPM dyes by SPC (a. BG, b. BF, c. CV). The error bars represent the standard deviation of the replicates ($n = 3$).

The original colored solution was decolorized to be nearly transparent in the process. The dye DP increases with time and reach around 90% in 20 min at a certain concentration. At the same time point, the higher the SPC dosage is, the higher the dye DP is. From these facts, the optimal dosage of SPC was determined, which is 2.0 mL for BG, 0.5 mL for BF and 2.0 mL for CV. And the decolorization time was determined to be 20 min. It is worth to note that the DP of dyes is fairly high in 20 min, which suggests SPC is an effective oxidant for TPM dyes decolorization.

Temperature is another important parameters governing the SPC decomposition as well as the degradation of dye intermediate. BG, BF, and CV were decolorized by SPC at the different temperature. As shown in Fig. 4, at room temperature (20°C), about 80% of BG and BF, as well as 60% of CV, are quickly decolorized by SPC in 5 min. At the end of 20 min, the dye DP has averagely reached up to 96%. The DP keeps on increasing until a saturation point is reached, after which little DP change is found with further temperature rise. It is suggested that in the range of 20–90°C, the higher the reaction temperature is, the sooner the maximum DP is achieved. While high temperature is conducive to SPC decomposition to H_2O_2, the release of HOO^- from H_2O_2 is accelerated, leading to a reduction in decolorization time. Considering easy practical operation, room temperature (20°C) was adopted in this work.

3.2. The decolorization of TPM@SiO_2 microspheres by SPC

The TPM-doped silica microspheres were synthesized by the Stöber method and characterized using UV-Vis, IR, and TEM techniques (In Support information). The TEM images (Fig. S2) show that the prepared TPM@SiO_2 is in a regular spherical shape with an average diameter of 200 –250 nm. The IR spectra of TPM@SiO_2 (Fig. S3) are in good agreement with the silica gel standard spectra, and also consistent with the IR spectra of nanosilica reported in the literature [29]. The good incorporation of TPM dyes and silica nanoparticles is combinedly demonstrated by the IR and UV-Vis spectra of bare TPM dyes, SiO_2 and TPM@SiO_2 (Fig. S4).

The synthesized TPM@SiO_2 microspheres were decolorized by SPC. The fairly high DP was obtained for all TPM@SiO_2 microspheres as shown in Table 1. The slight DP difference between three TPM@SiO_2 microspheres is due to their structural differences. It was found that, though under the action of five-fold dosage of SPC, the DP of TPM@SiO_2 microspheres is still lower than that of the corresponding bare dye in the same decolorization time. This suggests the interaction between SPC and dye is somewhat obstructed by the doped silica nanoparticles.

To further verify the decolorization performance of SPC to TPM@SiO_2 microspheres, the water-based inks were made by adding TPM@SiO_2 microspheres with different auxiliaries into an emulsion. It was observed that all three inks were significantly decolorized by SPC (Fig. S5). That means the TPM@SiO_2 microspheres as pigments in aqueous inks exhibit good fading effect under the action of SPC. These results also prove a possible alternative to sodium hydroxide with SPC in pulp bleaching [30].

In addition, the practicability of SPC oxidation to dye and dye-doped silica microspheres was testified. The simulated wastewater experiment was carried out under the preceding optimized conditions, and the fairly high removal efficiency of 86.23% for BG, 81.52% for BF, 75.65% for CV, 78.55% for BG@SiO_2, 73.83% for BF@SiO_2 and 68.12% for CV@SiO_2 were obtained.

Table 1
Decolorization effect of TPM dyes and TPM@SiO_2 microspheres by SPC

Project	BG	BG@SiO_2	BF	BF@SiO_2	CV	CV@SiO_2
t/min	20	20	20	20	20	20
V_{SP}/mL	1.0	5.0	1.0	5.0	1.0	5.0
DP/%	95	94	93	90	85	85

3.3. Mechanism analysis of TPM dyes oxidization by SPC

An obvious dye decolorization with the addition of SPC was observed in solution. The UV-Vis spectra of this variation are shown in Fig. 5. The maximum absorbance of BG, BF, and CV is at 624 nm, 542 nm, and 590 nm respectively,which is addressed to the characteristic absorption of the conjugated π bonding system in TPM molecule. With the adding of SPC, the characteristic absorption exhibits a decreasing trend to a negligible level, which could be is attributed to the HOO^- attack on the central carbon leading to the cleavage of conjugated bonds in TPM molecule. Because the conjugated structure of chromophore

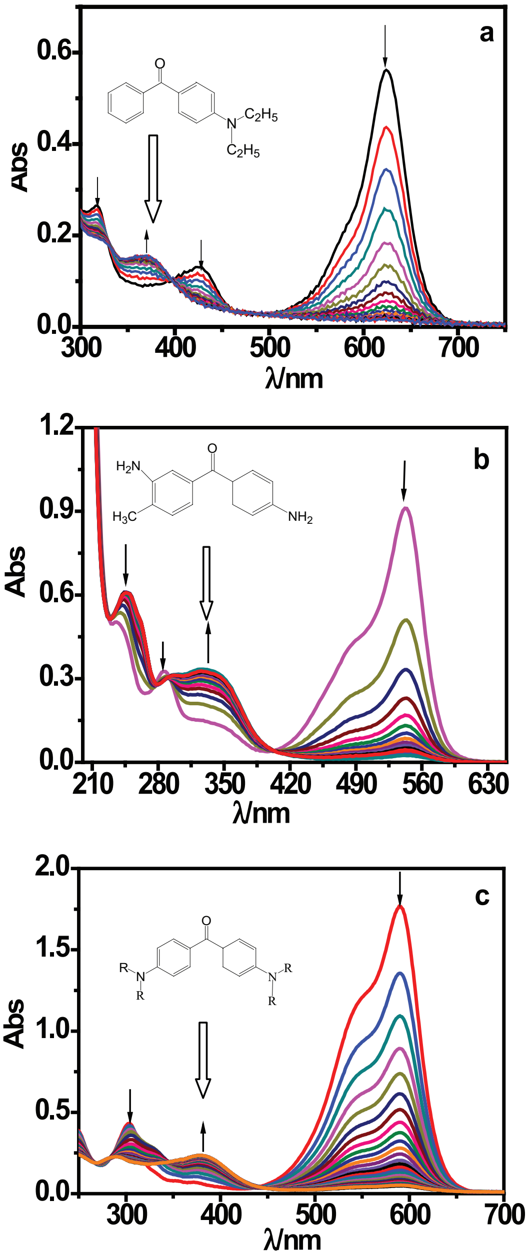

Fig. 5. The UV-Vis spectra change of TPM dyes by adding SPC at 2 min interval (a. BG, b. BF, c. CV).

is destructed in the process, the TPM dyes are effectively decolorized in this way. In addition, the cracking of conjugate structure in the dye molecule is also indicated by the decreasing absorption of BG at 426 nm and 318 nm.

At the same time, a slight blue shift of the maximum absorption is notable in the UV-Vis spectra of BG and CV, which is possibly due to N-dealkylation, i.e., the non-selective attack on C-N bond by reactive oxygen species in the oxidation process. As the alkyl groups are removed one by one, the formation of a series of N-dealkylated intermediates is in a stepwise manner [31]. Moreover, the characteristic absorption peak of benzene ring at 287 nm for BF and 303 nm for CV was observed to gradually decrease with time, which indicates the benzene rings are oxidized by SPC [32].

As the degradation proceeding, a new absorption peak appears at 370 nm, 325 nm, and 380 nm in the UV-Vis spectra of BG, BF and, CV respectively, and the absorption intensity is increased with time. This spectral change could be attributed to that new products is generated in the nucleophilic addition with the destruction of the conjugated structure in the dye molecule. Based on the UV-Vis spectra and literature, the main new products were deduced to bebenzophenone derivatives. From the benzophenone derivatives, some possible products in the subsequent degradation are derived [33], and the further reactions such as N-dealkylation, deamination, removal of the benzene ring and open ring reactions could be involved. All the ring-opening products could be eventually oxidized into small organic molecules, until ultimately mineralized into carbonate, nitrates, etc. In theory, all the above reactions are involved in the degradation of dye molecule [34].

The degradation of BG and CV could be mainly organized into the two parallel and competing reactions: HOO^- attack on the central carbon leading to the cleavage of conjugated bonds and N-dealkylation [35]. As there exists only one methyl group in BF molecular, and no significant shift of maximum absorption was observed in UV-Vis spectra, N-dealkylation should be excluded in the degradation of BF, and the major reaction is the HOO^- attack on the central carbon. Considering the above facts and all the experimental results, the following reaction mechanisms are proposed for the degradation of amino- or alkylamino-TPM (Fig. 6) by SPC.

The degradation of the three dyes was carried out under the optimized conditions, and the high DP of 95%, 93% and 85% was recorded for BG, BF, and, CV respectively (Table 1). The DP is ordered as BG > BF > CV under the same selected conditions. The slight DP difference among the three dyes may be attributed to the number and distribution of substituent in TMP structure. It is noted that three N-substituents are evenly distributed in the three benzene rings of CV and BF molecules, while only two of three benzene rings are fused with N-substituents in BG molecule (Fig. 1). The more substituent may provide the greater steric hindrance to the HOO^- attack on central carbon. Therefore, the DP of BF and CV is lower than that of BG under the same conditions. Along this line, the substituents at the three phenylamino groups are six H- in BF molecule, while six methyl groups are at the corresponding positions in the CV molecule. The steric hindrance of the methyl group is obviously stronger than that of H- in the attack of HOO^- on central carbon. Therefore, the DP of CV is somewhat lower than that of BF under the same conditions.

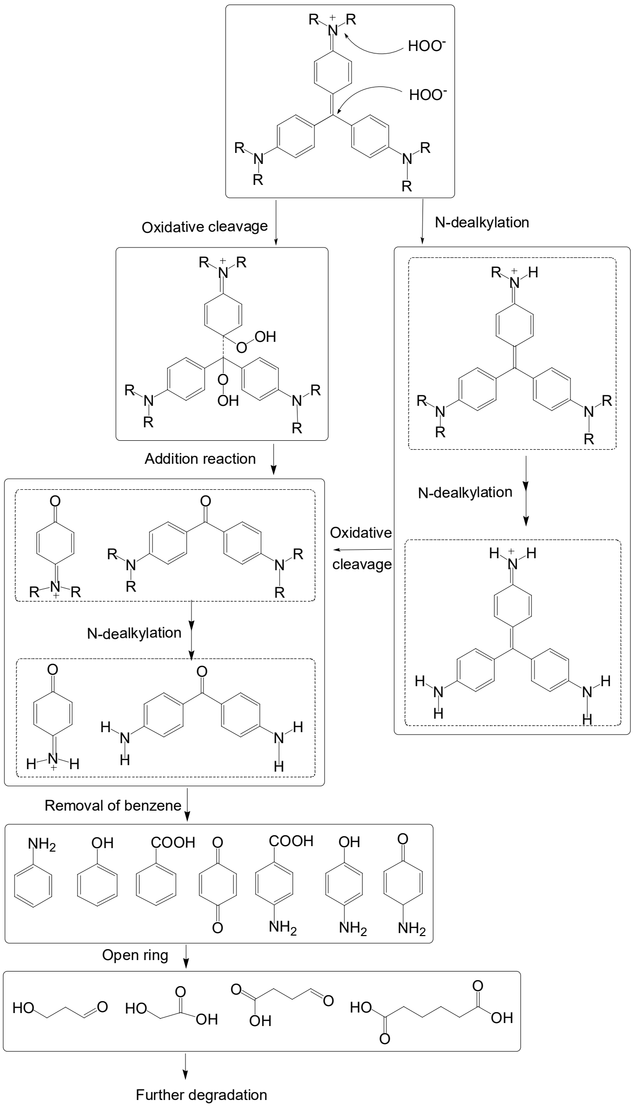

Fig. 6. The proposed degradation mechanism of Alkylamino-TPM dyes by SPC.

4. Conclusions

The TPM dyes of BG, CV, and BF were efficiently decolorized and degraded by SPC in the optimized conditions. Three TPM@SiO_2 microspheres were synthesized using the Stöber method and characterized by UV-Vis, IR and TEM analysis. The decolorization effect of the TPM@SiO_2 microspheres by SPC was identified to be a little weaker than that of the corresponding bare dyes. It is proposed that two main reactions are involved in the degradation of TPM dyes: the HOO^- attack on the central carbon leading to the broken of conjugate bonds in dye molecular, and the followed N-dealkylation. SPC was proved to be a practical oxidant for the degradation of amino- or alkylamino-TPM dyes. In general, the present work exploited a low cost and simple handling method for the removal of certain kinds of TPM dyes in aqueous solution, which offers potential application in the treatment of TPM dyes wastewater.

Acknowledgment

This work was supported by grants from the National Natural Science Foundation of China (No. 21575084), the Nature Science Foundation of Shanxi Province of China (No. 201601D102009).

References

[1] X. Zhao, R.P. Bagwe, W. Tan, Development of organic-dye-doped silica nanoparticles in a reverse microemulsion, Adv. Mater., 16 (2004) 173–176.

[2] J.E. Lee, N. Lee, H. Kim, J. Kim, S.H. Choi, J.H. Kim, T. Kim, I.C. Song, S.P. Park, W.K. Moon, T. Hyeon, Uniform mesoporous dye-doped silica nanoparticles decorated with multiple magnetite nanocrystals for simultaneous enhanced magnetic resonance imaging, fluorescence imaging, and drug delivery, J. Am. Chem. Soc., 132 (2009) 552–557.

[3] P. Yu, J. He, C. Guo, 9-Thiourea Cinchona alkaloid supported on mesoporous silica as a highly enantioselective, recyclable heterogeneous asymmetric catalyst, Chem. Commun., 20 (2008) 2355–2357.

[4] J. Yu, L. Zhao, B. Cheng, Preparation of monodispersed microporous SiO_2 microspheres with high specific surface area using dodecylamine as a hydrolysis catalyst, J. Solid State Chem., 179 (2006) 226–232.

[5] C. Wang, Q. Ma, W. Dou, S. Kanwal, G. Wang, P. Yuan, X. Su, Synthesis of aqueous CdTe quantum dots embedded silica nanoparticles and their applications as fluorescence probes, Talanta, 77 (2009) 1358–1364.

[6] R.D. Soltani, A.R. Khataee, M. Safari, S.W. Joo, Preparation of bio-silica/chitosan nanocomposite for adsorption of a textile dye in aqueous solutions, Int. Biodeter. Biodegr., 85 (2013) 383–391.

[7] Y. Zhang, Y. Zhang, X. Fei, L. Yu, B. Zhang, Preparation and characterisation of silica supported organic hybrid pigments, Pigm. Resin Technol., 43 (2014) 325–331.

[8] M. Zhao, Z. Tang, P. Liu, Removal of methylene blue from aqueous solution with silica nano-sheets derived from vermiculite, J. Hazard. Mater., 158 (2008) 43–51.

[9] S. Nouren, H.N. Bhatti, Mechanistic study of degradation of basic violet 3 by Citrus limon peroxidase and phytotoxicity assessment of its degradation products, Biochem. Eng. J., 95 (2015) 9–19.

[10] X. Yang, J. Zheng, Y. Lu, R. Jia, Degradation and detoxification of the triphenylmethane dye malachite green catalyzed by crude manganese peroxidase from Irpex lacteus, Environ. Sci. Pollut. R., 23 (2016) 9585–9597.

[11] N. Modirshahla, M.A. Behnajady, Photooxidative degradation of Malachite Green (MG) by UV/H_2O_2: Influence of operational parameters and kinetic modeling, Dyes Pigm., 70 (2006) 54–59.

[12] Y. Ju, S. Yang, Y. Ding, C. Sun, C. Gu, Z. He, C. Qin, H. He, B. Xu, Microwave-enhanced H_2O_2-based process for treating aqueous malachite green solutions: intermediates and degradation mechanism, J. Hazard. Mater., 171 (2009) 123–132.

[13] Y. Ju, S. Yang, Y. Ding, C. Sun, A. Zhang, L. Wang, Microwave-assisted rapid photocatalytic degradation of malachite green in TiO_2 suspensions: mechanism and pathways, J. Phys. Chem. A, 112 (2008) 11172–11177.

[14] S. Wang, Y. Guan, L. Wang, W. Zhao, H. He, J. Xiao, S. Yang, C. Sun, Fabrication of a novel bifunctional material of BiOI/Ag_3VO_4 with high adsorption-photocatalysis for efficient treatment of dye wastewater, Appl. Catal., B, 168–169 (2015) 448–457.

[15] J. Li, H. Zhang, Y. Hao, Ying Chen, Decoloration of triphenylmethane dyes wastewater by potassium ferrate (in Chinese), Ind. Water. Wastewater, 2 (2013) 27–29.

[16] L.M.A. Fayoumi, M.A. Ezzedine, H.H. Akel, M.M. El Jamal, Kinetic study of the degradation of crystal violet by $K_2S_2O_8$. Comparison with Malachite Green, Port Electrochim. Acta, 30 (2012) 121–133.

[17] M. Hamza, R. Abdelhedi, E. Brillas, I. Sirés, Comparative electrochemical degradation of the triphenylmethane dye Methyl Violet with boron-doped diamond and Pt anodes, J. Electro-Anal. Chem., 627 (2009) 41–50.

[18] I. Sirés, E. Guivarch, N. Oturan, M.A. Oturan, Efficient removal of triphenylmethane dyes from aqueous medium by in situ electrogenerated Fenton's reagent at carbon-felt cathode, Chemosphere, 72 (2008) 592–600.

[19] L. Yong, G. Zhanqi, J. Yuefei, H. Xiaobin, S. Cheng, Y. Shaogui, W. Lianhong, W. Qingeng, F. Die, Photodegradation of malachite green under simulated and natural irradiation: kinetics, products, and pathways, J. Hazard. Mater., 285 (2015) 127–136.

[20] G. Cravotto, S. Di Carlo, B. Ondruschka, V. Tumiatti, C.M. Roggero, Decontamination of soil containing POPs by the combined action of solid Fenton-like reagents and microwaves, Chemosphere, 69 (2007) 1326–1329.

[21] F.J. Rivas, O. Gimeno, T. Borralho, M. Carbajo, UV-C radiation based methods for aqueous metoprolol elimination, J. Hazard. Mater., 179 (2010) 357–362.

[22] A.C. Herath, R.M. Rajapakse, A. Wicramasinghe, V. Karunaratne, Photodegradation of triphenylamino methane (magenta) by photosensitizer in oxygenated solutions, Environ. Sci. Technol., 43 (2008) 176–180.

[23] R. Ohura, A. Katayama, T. Takagishi, Decoloration of natural coloring matter with sodium percarbonate, Text. Res. J., 61 (1991) 242–246.

[24] A. McKillop, W.R. Sanderson, Sodium perborate and sodium percarbonate: cheap, safe and versatile oxidising agents for organic synthesis, Tetrahedron, 51 (1995) 6145–6166.

[25] Y. Imabayashi, R. Kobayashi, S. Yoshikawa, Studies on bleaching action of oxidizing bleaching agent (part 2): protecting effect of tannic acid on the degradation and decolorization of the fabric dyed with metalized (Cu) dye in bleaching process, Bull. Fac. Home. Life. Sci. Fukuoka. Womens. U., 17 (1985) 17–23.

[26] J. Li, Y. Xue, J. He, Study on the degradation of rhodamine by sodium percarbonate (in Chinese), Environ. Eng., S2 (2012) 176–178.

[27] B. Yang, J.J. Pignatello, D. Qu, B. Xing, Activation of hydrogen peroxide and solid peroxide reagents by phosphate ion in alkaline solution, Environ. Eng. Sci., 33 (2016) 193–199.

[28] K.M. Thompson, W.P. Griffith, M. Spiro, Mechanism of bleaching by peroxides. Part 1.-Kinetics of bleaching of phenolphthalein by hydrogen peroxide at high pH, J. Chem. Soc., Faraday Trans., 89 (1993) 4035–4043.

[29] V.M. Gun'ko, V.V. Turov, V.N. Barvinchenko, V.M. Bogatyrev, A.V. Turov, O. Shulga, R. Leboda, V.G. Sukretny, B.A. Chuikov, Y.G. Ptushinskii, Characteristics of interfacial water at nanosilica surface with adsorbed 1,3,5-trihydroxybenzene over wide temperature range, Colloids Surf., A, 278 (2006) 106–122.

[30] C. Leduc, M. Garceau, C. Daneault, S. Robert, Bleaching of a mechanical pulp with sodium percarbonate and amineborane: Bleaching response and brightness stability, J. Pulp Pap. Sci., 28 (2002) 171–175.

[31] C.C. Chen, C.S. Lu, Y.C. Chung, J.L. Jan, UV light induced photodegradation of malachite green on TiO_2 nanoparticles, J. Hazard. Mater., 141 (2007) 520–528.

[32] L. Shi, X. Wang, N. Li, C. Huai, J. Liu, UV irradiation chlorine dioxide photocatalytic oxidation of simulated fuchsine wastewater by UV-Vis and online FTIR spectrophotometric method, ISRN Anal. Chem., (2012) 1–7.

[33] S. Asad, M.A. Amoozegar, A. Pourbabaee, M.N. Sarbolouki, S.M. Dastgheib, Decolorization of textile azo dyes by newly isolated halophilic and halotolerant bacteria, Bioresource. Technol., 98 (2007) 2082–2088.

[34] D.F. Duxbury, The photochemistry and photophysics of triphenylmethane dyes in solid and liquid media, Chem. Rev., 93 (1993) 381–433.

[35] C.C. Chen, F.D. Mai, K.T. Chen, C.W. Wu, C.S. Lu Photocatalyzed N-de-methylation and degradation of crystal violet in titania dispersions under UV irradiation, Dyes Pigm., 75 (2007) 434–442.

Support information

1. Screening of dyes by sodium percarbonate (SPC)

Eight kinds of basic dyes including malachite green, brilliant green (BG), basic fuchsin (BF), crystal violet (CV), methyl violet, victoria blue B, methylene blue and safranine T) – two kinds of acid dyes (acid fuchsin and methyl blue), seven kinds of reactive dyes (reactive orange, reactive blue, reactive black, reactive dark red, reactive dark blue, reactive navy blue and reactive dark yellow) were used to prepare solutions of 100 mg/L respectively. SPC solution (1 mL, 50 mg/L) was added into a colorimetric tube containing dye solution (1 mL) and the fading of the dye solution was observed. The degradable dye was screened out.

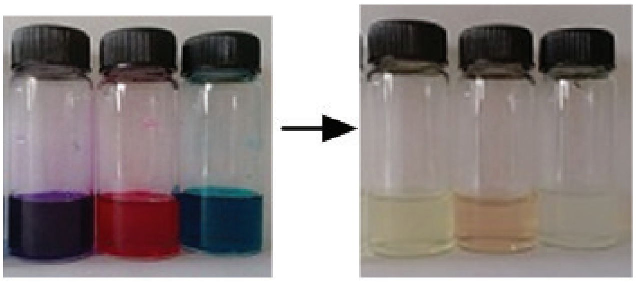

Fig. S1. The color change of dyes in the decolorization by SPC. (From left to right: CV, BF and BG).

2. Synthesis of nano-silica and TPM@SiO$_2$ microspheres

Water (1.2 mL) and 3 mL of ammonia were added to 60 mL of absolute ethanol. After 3 mL of ethyl orthosilicate was added dropwise, the mixture was heated and stirred at 50°Cfor 24 h continuously. Then the mixture was centrifuged and washed with ethanol and redistilled water. After vacuum drying at 25°C for 24 h, the solid was collected.

Dye (0.5 g) was added to 60 mL of ethanol. The mixture was stirred for 5 min. After then, 1.2 mL of water and 3 mL

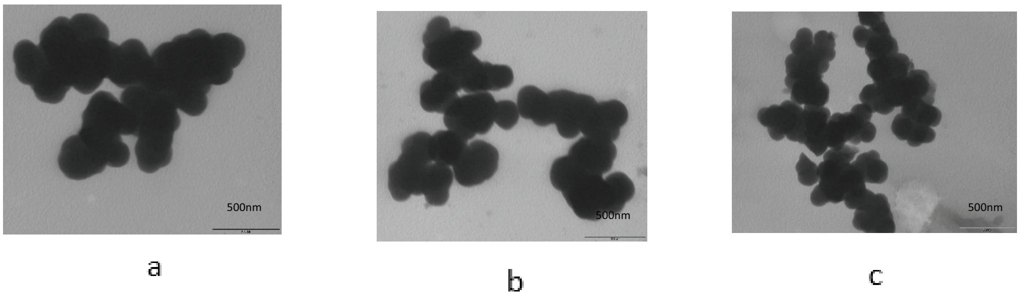

Fig. S2. The TEM images of the dye-doped silica microspheres (a. SiO$_2$@BG, b. SiO$_2$@BF, c. SiO$_2$@CV).

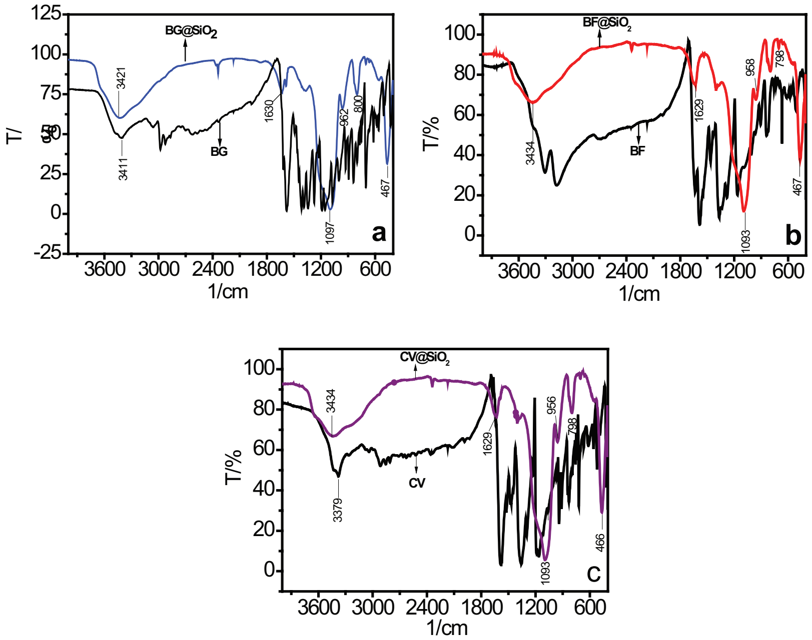

Fig. S3. The IR spectra of BG, BF and CV before and after silica-nanoparticles doping.

of aqueous ammonia were added. After 3 mL of ethyl orthosilicate was dropwisely added, the mixture was heated and stirred at 50°C for 24 h continuously. Then the mixture was centrifuged and washed with ethanol and redistilled water. After vacuum drying at 25°C for 24 h, the colored solid was collected.

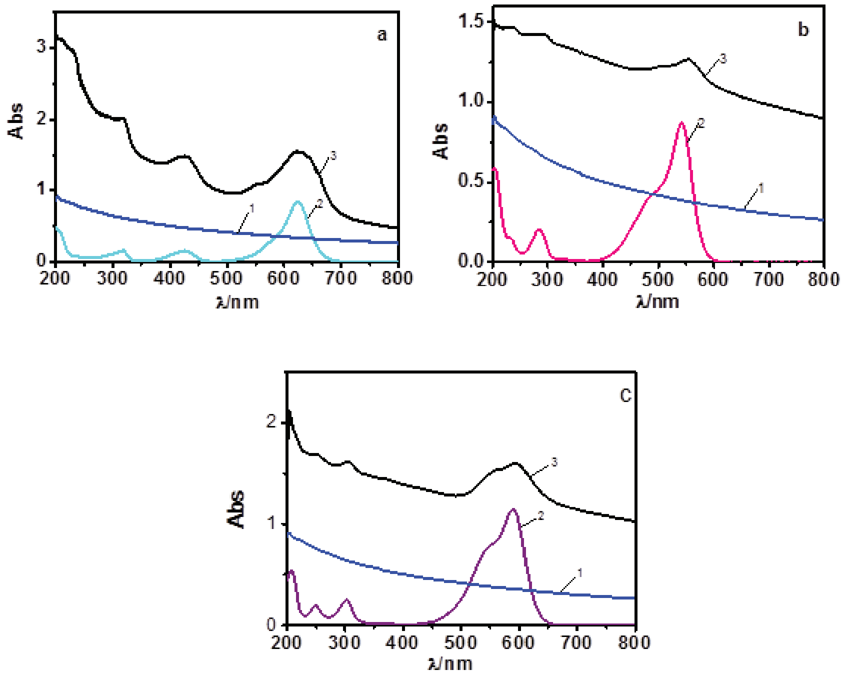

Fig. S4. The UV-Vis spectra of a. BG, b. BF, c. CV in which 1. SiO_2, 2. Dye and 3. TPM@SiO_2.

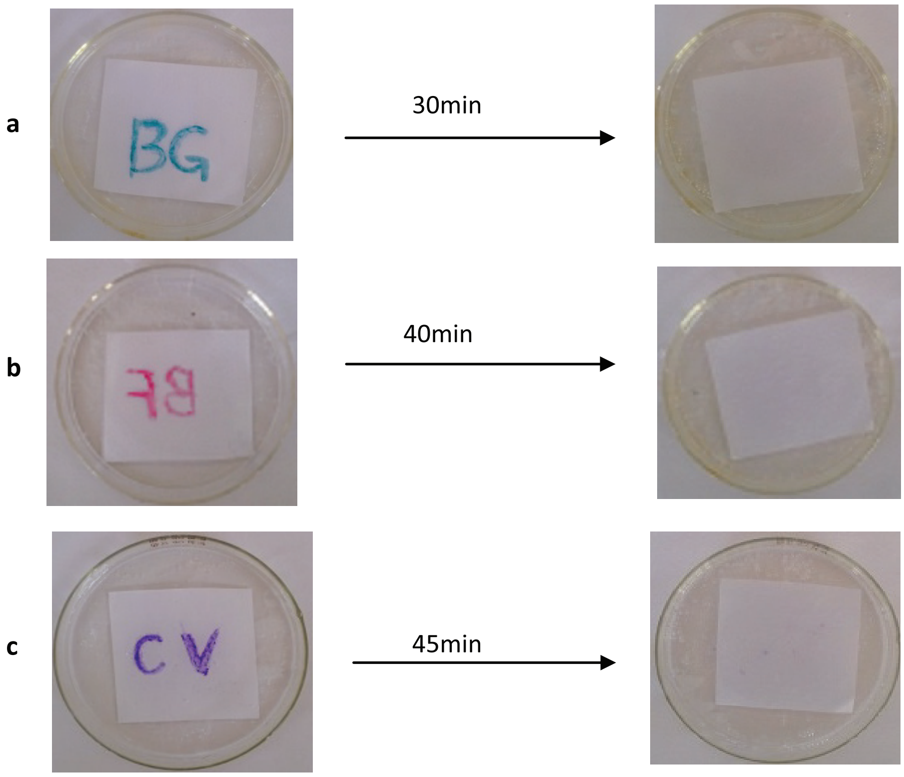

Fig. S5. The decolorization of aqueous TPM@SiO_2 microspheres inks by SPC (a. BG@SiO_2, b. BF@SiO_2, c. CV@SiO_2).